

Dual-Energy-based Beam Hardening Correction in Digital Volume Tomography (DVT)

S. Schüller^{1,2,3}, K. Stannigel³, M. Hülsbusch³, S. Sawall^{1,2},
J. Ulrici³, E. Hell³ and M. Kachelrieß^{1,2}

¹Medical Physics in Radiology, German Cancer Research Center (DKFZ), Heidelberg, Germany

²Institute of Medical Physics, Friedrich-Alexander-University (FAU), Erlangen, Germany

³Sirona Dental Systems GmbH, Bensheim, Germany

Purpose

In digital volume tomography (DVT) the image quality often suffers from beam hardening (BH) artifacts. The artifacts appear in the vicinity of strong attenuating objects like bones, teeth or implants which are densely positioned in the dentition. The polychromatic nature of x-ray radiation causes the BH artifacts. Several publications [1-3] have shown that suitable combinations of the low- and high-energy images of a dual-energy scan can provide images with different image characteristics like reduced BH and metal artifacts as well as an improved contrast-to-noise ratio (CNR). However, the solutions are mutually exclusive and only one parameter can be optimized at the same time. For example metal artifact reduced images always suffer from high noise [4] and require post-processing by noise reduction techniques like adaptive filtering, which might degrade spatial resolution. In the dental field, a special need for high spatial resolution and high contrasts exists [5].

State-of-the-art DVTs perform at high spatial resolution ($\approx 100 \mu\text{m}$) [6] to visualize dental structures correctly. Each BH reduction technique leading to a blurring or a contrast reduction is not acceptable especially for dental diagnostics.

Materials and Methods

To minimize BH artifacts we utilize the fact that BH occurs with different strength in the low- and high-energy images. By using a linear weighting between these images, the artifacts can be significantly reduced. This kind of weighting, however, leads to increased image noise (fig. 1) and a decrease of the CNR (fig. 9) in the resulting BH-reduced image. To overcome this issue we propose a voxel-wise non-linear blending (fig. 5) between the soft-tissue regions of the previously generated BH-reduced image and the strong attenuating regions, e.g. teeth, of the low-energy image which shows a good contrast. After all, the combination of the low frequencies of the non-linear blended image and the high frequencies of a minimal noise image (fig. 6) re-establishes fine structures and low image noise (fig. 8). A schematic overview of the algorithm is presented in figure 2. The proposed algorithm performs in image domain because the angular sampling between the two dual-energy scans might differ. If not noted otherwise all reconstructions are performed using a filtered backprojection, in our case the Feldkamp-Davis-Kress (FDK) [7] reconstruction without any further post-processing.

Data Acquisition: Cadaver heads were scanned on a Galileos DVT (Sirona, Bensheim, Germany). Each scan was performed over an angular range of 210° and the number of projections was 200 per scan.

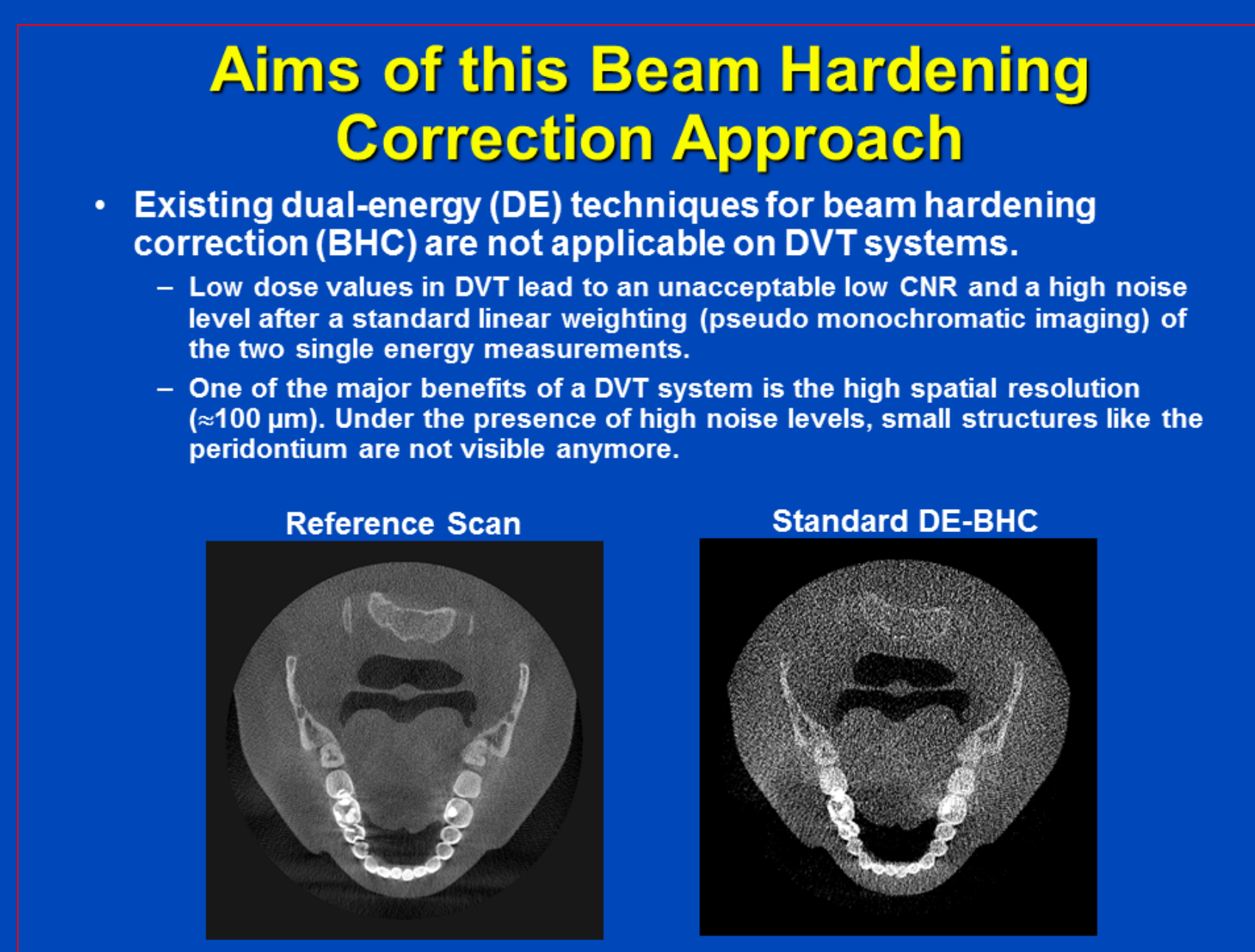


Figure 1: State-of-the-art beam hardening correction techniques and challenges for a dual-energy DVT system.

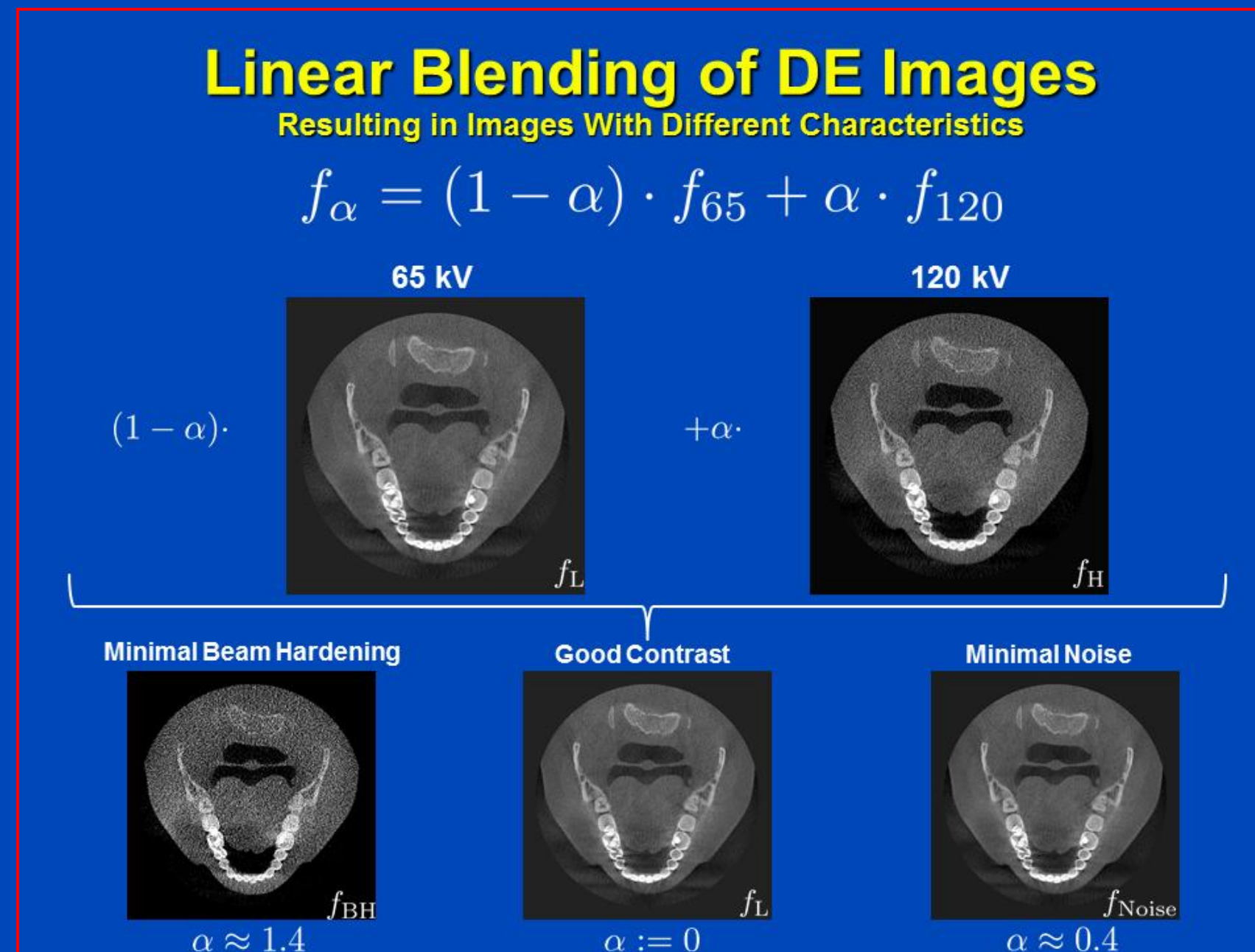


Figure 3: Different linear α -blendings of the low (65 kV) and the high (120 kV) energy images resulting in images with different characteristics like minimal beam hardening, good contrast and minimal noise. (C=500 HU, W=3000 HU)

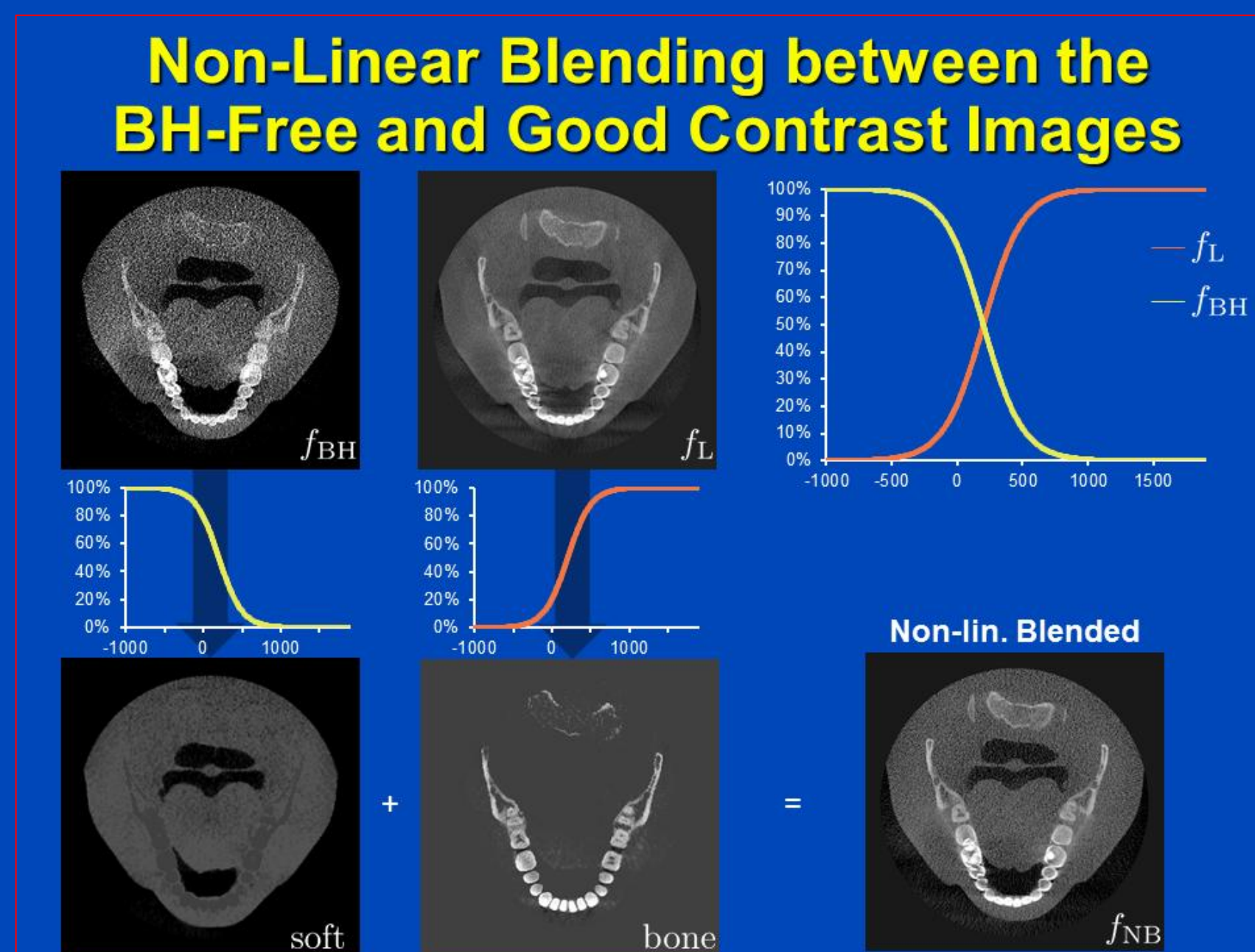


Figure 5: Non-linear blending of the noisy BH-reduced image and the good contrast image. The final blended image is a combination of the resulting soft tissue and bone images.

Contrast-to-Noise (CNR) Analysis

	Soft Tissue		Bone		CNR
	Mean	Noise	Mean	Noise	
f_{Ref}	133 HU	277 HU	1358 HU	334 HU	2.83
f_L	68 HU	97 HU	1459 HU	132 HU	5.98
f_H	137 HU	170 HU	1065 HU	197 HU	2.58
f_{Noise}	83 HU	86 HU	1376 HU	114 HU	6.41
f_{BH}	195 HU	294 HU	823 HU	344 HU	1.00
f_{NB}	175 HU	256 HU	1455 HU	134 HU	3.14
f_{FS}	181 HU	84 HU	1446 HU	111 HU	6.45

The complete dual-energy scan has the same dose level as the 98 kV reference scan.

Volume regions for bone and soft tissue to measure noise, contrast and CNR.

Figure 7: An overview of CNR levels for the intermediate resulting images, the reference image f_{Ref} and the final image f_{FS} . The ROIs to measure mean and noise inside the soft tissue and the bone are indicated at the bottom.

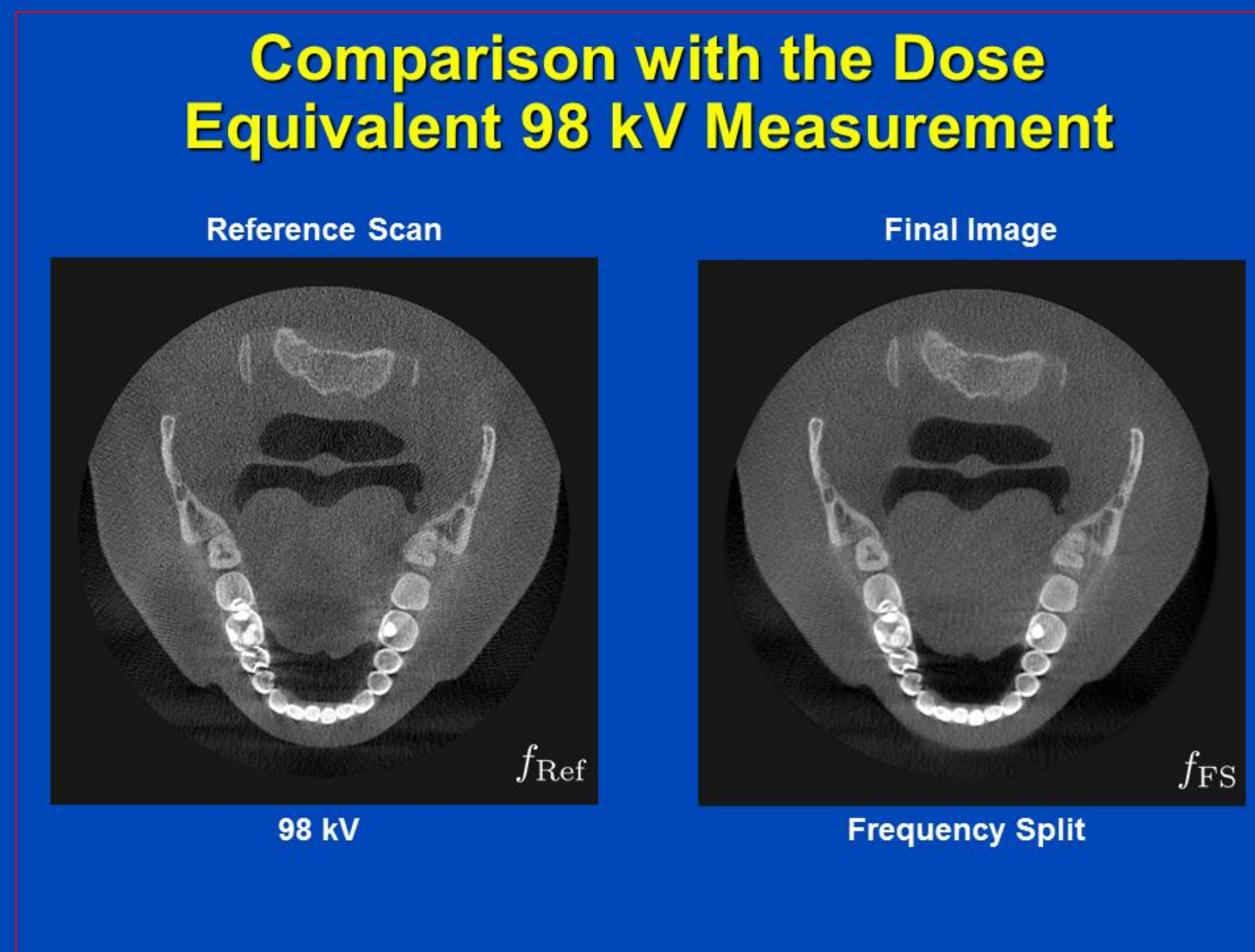


Figure 9: Direct comparison of the final beam hardening reduced image of the new approach and the 98 kV reference image.

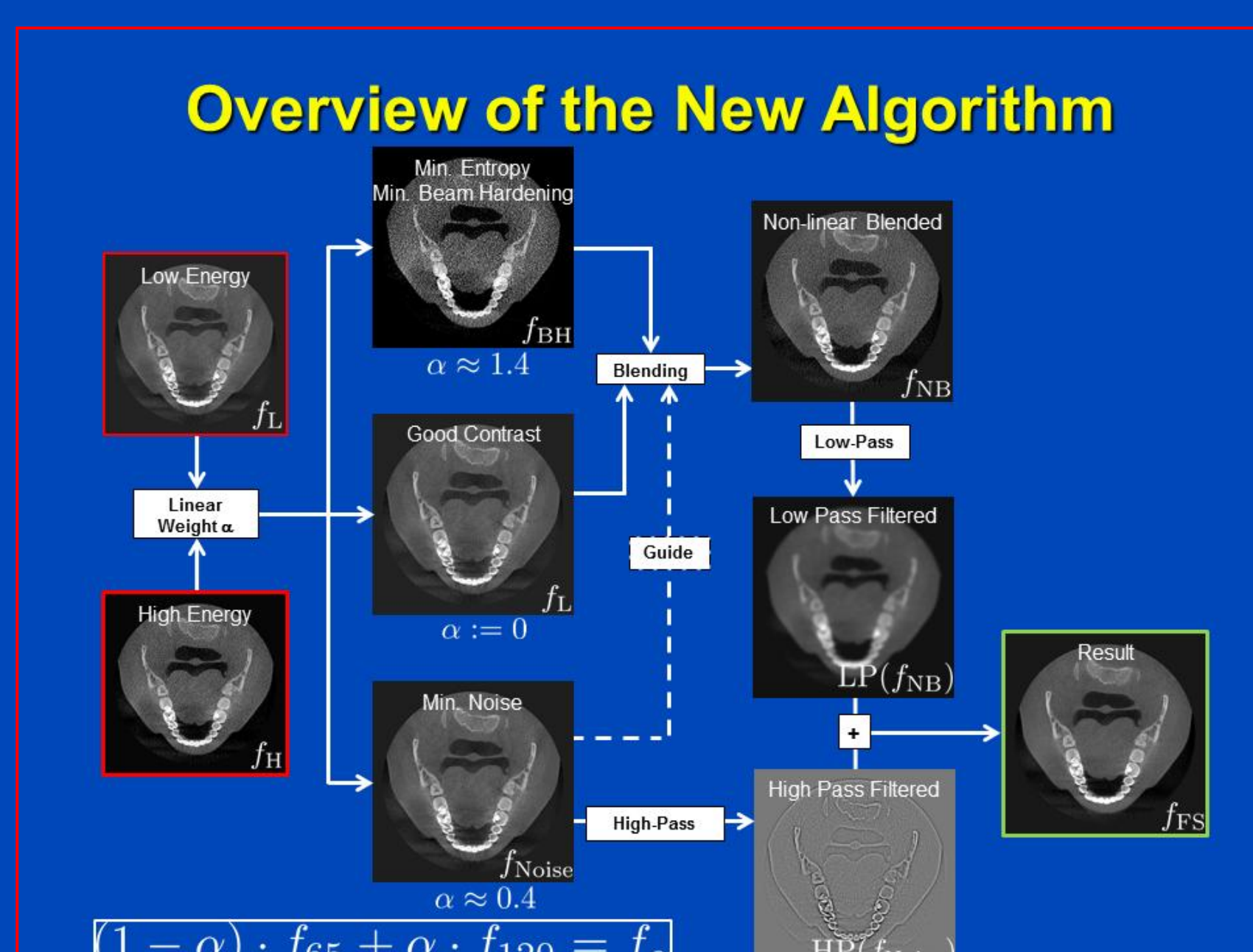


Figure 2: Block diagram of the whole algorithm. Linear weighting of f_L and f_H generating f_{BH} , f_L , and f_{Noise} . f_{Noise} is used as a guide for the non-linear blending of f_L and f_{BH} . The final image f_{FS} is generated by a voxel-wise summation of the high pass of f_{Noise} and the low pass of f_{NB} .

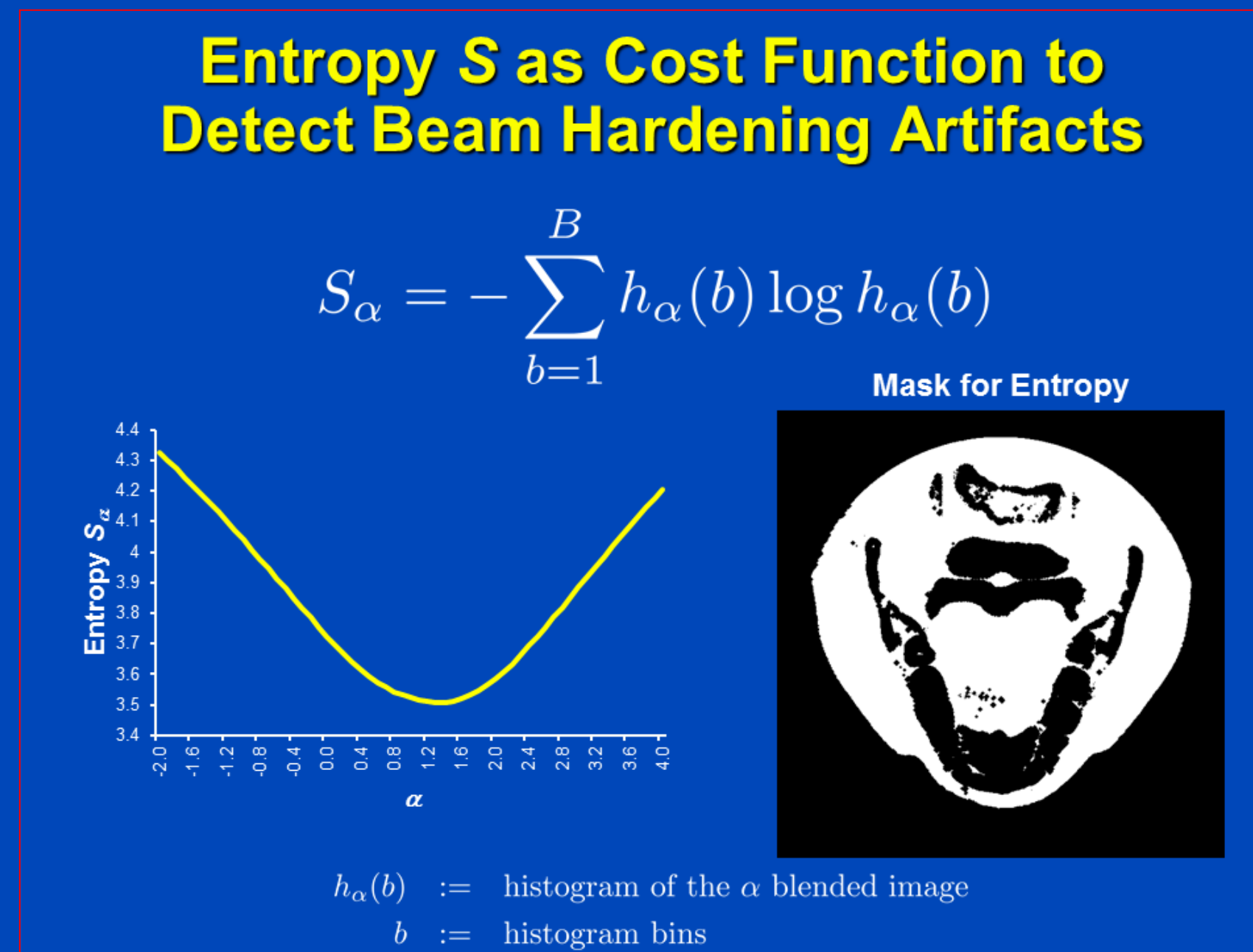


Figure 4: Left part of the figure illustrates the relation between Entropy S and the linear α -blending. The right hand-side shows the automatic calculated soft-tissue mask which is used to estimate the amount of beam hardening.

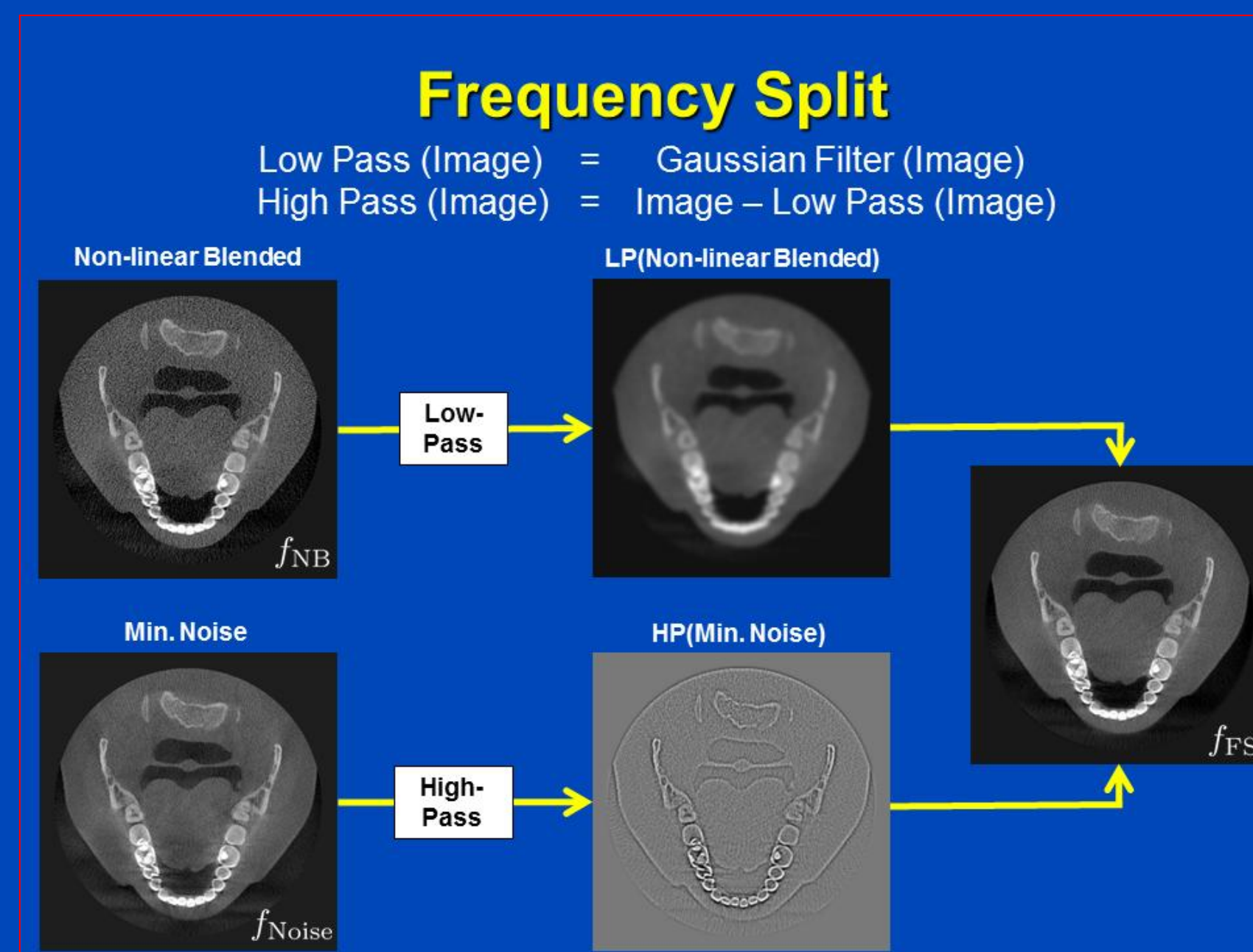


Figure 6: Illustration of frequency split of the non-linear blended BH-reduced and the minimal noise image. This operation is performed in the image domain by applying a Gaussian filter.

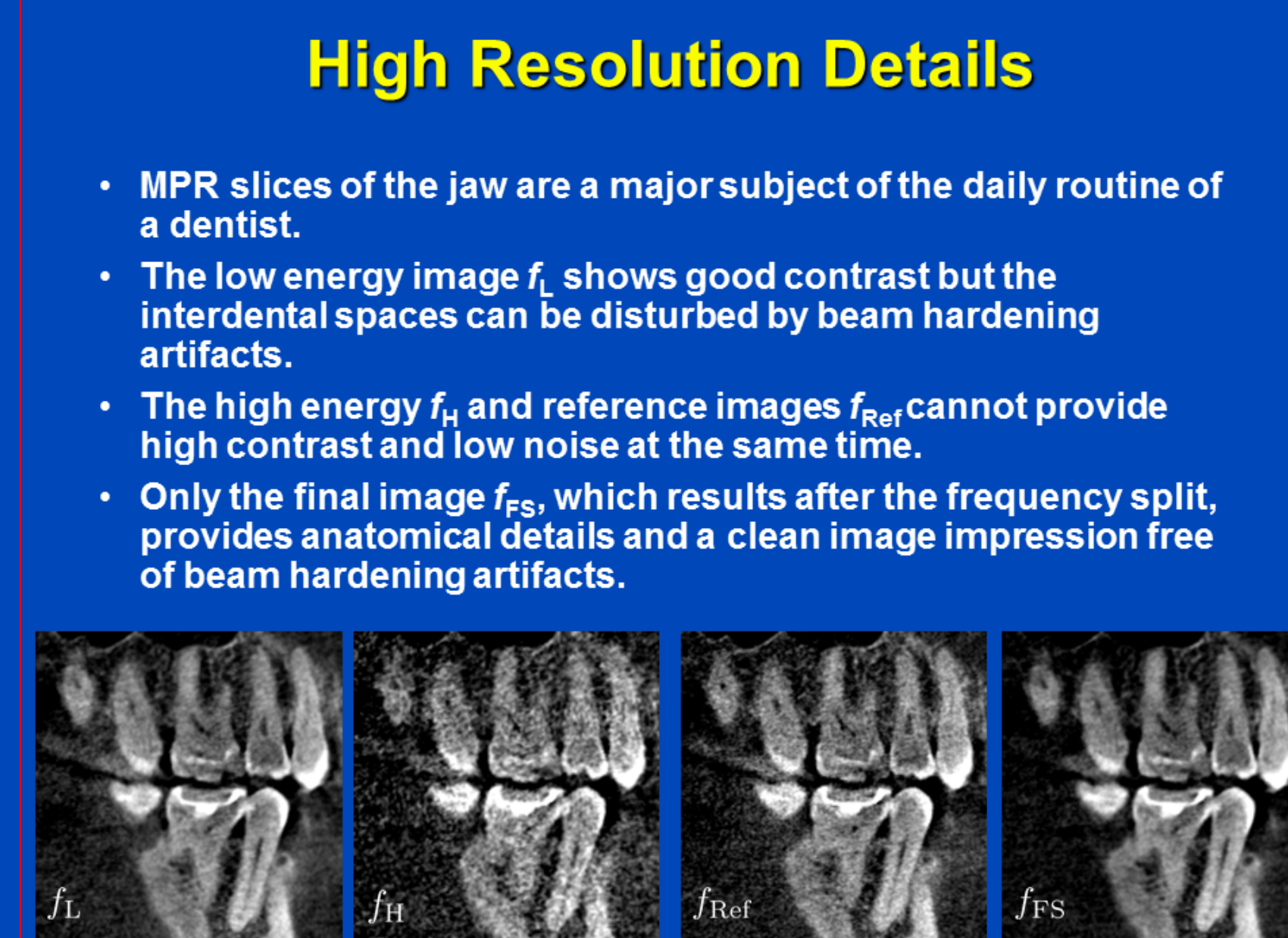


Figure 8: A common clinical case is a MPR along the jaw. Center and window are adapt for each image according to the contrasts inside the ROIs. The windowing corresponds to C=1500 HU, W=3000 HU of f_{Ref} . Voxel size $250 \mu\text{m}^3$.

Discussion

- Open parameters like the position of the non-linear blending transition and the frequency split filter can be automatically determined from the image histogram.
- The automatic soft tissue segmentation and the system-dependent but otherwise fix parameters allow for fully automatic image processing.
- Compared to the two initial image reconstructions, the post processing steps of filtering and non-linear blending are much less time consuming. Thus the algorithm can be performed easily for each dual-energy scan.
- The proposed approach fulfills the high demands of dental imaging:
 - The SNR is increased while the spatial resolution is maintained.
 - High contrasts, equivalent to the low (65 kV) image, are achieved.
 - The dose levels are comparable to state-of-the-art DVT protocols.

Figure 10: Short discussion of practicability of the proposed algorithm and the benefits of the dual-energy acquisition compared to a single-energy scan.

The following scans were performed:

- reference scan f_{Ref} : 98 kV, 12 mAs
- low energy f_L : 65 kV, 36 mAs
- high energy f_H : 120 kV, 18 mAs, Cu

For a better comparison all images are without post-processing. The dual-energy scan has the same total dose as the reference scan.

Results

Fig. 8 and 9 illustrate the potential of the proposed BH artifact reduction for DVT. The reduction of the streaks can also be seen in tiny spaces between the teeth, where a diagnosis can be strongly affected by this kind of artifacts. The number and magnitude of the BH streaks has decreased in the final image in comparison to the low and high energy images. The ROIs for the CNR evaluations are depicted in fig. 7. Arrows pointing in fig. 9 to regions which benefit from the proposed BH reduction algorithm.

A short overview of noise, contrast and CNR for the basis and final images are presented in fig. 7. The proposed method achieves the highest CNR compared to the reference scan at 98 kV and the two single scans of the dual-energy scan. This is a consequence of the properties of the non-linear blending, which assures the high contrast of low energy image and the frequency split, which in an ideal case only contains the low noise level of the minimal noise image also achieved by linear weighting. This leads to a CNR outperforming all 3 initial reconstructions.

Conclusion

The herein proposed method can easily and automatically reduce beam hardening artifacts in DVT routine and the results indicate that it is superior to previously published BH-correction [6] algorithms in terms of noise and dose usage. The spatial resolution which plays an important role for the dentist is not degraded by the new algorithm. It can also be noticed that reduced noise and BH in the proximity of bone and teeth structures clearly improve the capabilities for the diagnostics. As a result of the higher CNR, a dose reduction for some applications could also be possible and leads to a increased patient safety.

References

- A. Coleman and M. Sinclair, "A beam-hardening correction using dual-energy computed tomography," *Physics in Medicine and Biology*, vol. 30, no. 11, p. 1251, May 1985.
- F. Bamberg et al., "Metal artifact reduction by dual energy computed tomography using monoenergetic extrapolation," *European Radiology*, vol. 21, no. 7, pp. 1424-1429, Jan. 2011.
- D. R. Holmes III et al., "Evaluation of non-linear blending in dual-energy computed tomography," *European Journal of Radiology*, vol. 68, no. 3, pp. 409-413, Dec. 2008.
- L. Yu, S. Leng, and C. H. McCollough, "Dual-Energy CT-Based Monochromatic Imaging," *American Journal of Roentgenology*, vol. 199, no. 5, pp. S9-S15, Sep. 2012.
- C. Holberg et al., "Cone-beam computed tomography in orthodontics: benefits and limitations," *Journal of Orofacial Orthopedics/Fortschritte der Kieferorthopädie*, vol. 66, no. 6, pp. 434-444, Sep. 2005.
- Y. Kyriakou et al., "Digital volume tomography (DVT) and multislice spiral CT (MSCT): an objective examination of dose and image quality," in *RöFo. Fortschritte auf dem Gebiet der Röntgenstrahlen und der bildgebenden Verfahren*, vol. 183, no. 02, pp. 144-153, Oct. 2010.
- L. Feldkamp, L. Davis, and J. Kress, "Practical cone-beam algorithm," *Journal of the Optical Society of America*, vol. 1, no. 6, pp. 612-619, Jun. 1984.

Send correspondence request to:
Sören Schüller
soeren.schueller@dkfz.de
German Cancer Research Center (DKFZ)
Im Neuenheimer Feld 280
69120 Heidelberg, Germany

